



The impact of
periodization on the
energy spectra

V. Blažica et al.

This discussion paper is/has been under review for the journal Geoscientific Model Development (GMD). Please refer to the corresponding final paper in GMD if available.

The impact of periodization methods on the kinetic energy spectra for limited-area numerical weather prediction models

V. Blažica^{1,*,**}, N. Gustafsson², and N. Žagar¹

¹Department of Physics, Faculty of Mathematics and Physics, University of Ljubljana, Ljubljana, Slovenia

²Swedish Meteorological and Hydrological Institute, Norrköping, Sweden

* now at: Slovenian Environment Agency, Ljubljana, Slovenia

** Invited contribution by V. Blažica, recipient of the EGU Outstanding Student Poster Award 2013.

Received: 14 August 2014 – Accepted: 17 September 2014 – Published: 29 September 2014

Correspondence to: V. Blažica (vanja.blazica@gmail.com)

Published by Copernicus Publications on behalf of the European Geosciences Union.

Title Page	
Abstract	Introduction
Conclusions	References
Tables	Figures
⏪	⏩
◀	▶
Back	Close
Full Screen / Esc	
Printer-friendly Version	
Interactive Discussion	



Abstract

The paper deals with the comparison of the most common periodization methods used to obtain spectral fields of limited-area models for numerical weather prediction. The focus is on the impact the methods have on the spectra of the fields, which are used for verification and tuning of the models. A simplified model is applied with random fields that obey a known kinetic energy spectrum. The periodization methods under consideration are detrending, the discrete cosine transform and the application of an extension zone. For extension zone, three versions are applied: the Boyd method, the ALADIN method and the HIRLAM method. The results show that detrending and the discrete cosine transform have little impact on the spectra, as does the Boyd method for extension zone. For the ALADIN and HIRLAM methods, the impact depends on the width of the extension zone – the wider the zone, the more artificial energy and the larger impact on the spectra. The width of the extension zone correlates to the modifications in the shape of the spectra as well as to the amplitudes of the additional energy in the spectra.

1 Introduction

As the horizontal resolution of numerical weather prediction (NWP) models steadily increases, rigorous evaluation of the models' kinetic energy spectra at small scales becomes more important. At horizontal scales between a few hundred and a few km, which are the focus of mesoscale NWP models, statistical properties of turbulent motions in the upper troposphere and lower stratosphere have been shown to be consistent with the Kolmogorov scaling of turbulence defined by the energy dissipation rate. Scale distribution of turbulent motion energy is described by the $k^{-5/3}$ law, where k is the horizontal wavenumber. The scaling is horizontally nearly isotropic as it was confirmed in aircraft observations (e.g., Nastrom and Gage, 1985; Lindborg, 1999) and numerical model outputs.

GMDD

7, 6489–6518, 2014

The impact of periodization on the energy spectra

V. Blažica et al.

Title Page

Abstract

Introduction

Conclusions

References

Tables

Figures



Back

Close

Full Screen / Esc

Printer-friendly Version

Interactive Discussion



requires bi-periodicity of the prognostic fields which is in both models achieved by the so-called extension zone or E-zone (Haugen and Machenhauer, 1993). The application of the E-zone adds an additional belt of grid points in both x and y directions, in which the fields are periodized using trigonometric (HIRLAM) or spline functions (ALADIN).

5 Recently, the Boyd method (Boyd, 2005) was employed to the ALADIN model as well (Termonia et al., 2012; Degrauwe et al., 2012); the method uses infinitely differentiable windowing functions in the extension zone.

Two other periodization methods, which do not require the extension zone, are detrending (Errico, 1985) and the discrete cosine transform (DCT, Ahmed et al., 1974; Denis et al., 2002). The detrending method removes large-scale trends in each line and in each column of the grid-point field and it has been widely used for the computation of spectra. The DCT method creates a symmetric field by taking a mirror image of the original function. Neither of these two methods is suitable for the forecasting as they alter the values or size of the prognostic variables. Instead, they are used posteriori for the verification and tuning purposes (e.g., Skamarock, 2004; Ricard et al., 2013; Brousseau et al., 2012).

In the case of the ALADIN model and closely related models AROME and HARMONIE, the presence of the E-zone in the spectral computation assumes that the kinetic energy, added within the extension zone, does not have a significant impact on presented spectra. While this may apply to some levels and situations, it does not apply in general, as seen in Fig. 1a which compares kinetic energy spectra in the stratosphere in two experiments with everything the same except the width of the E-zone. It can be seen that the energy spectrum for the E-zone with a width around 50 km (i.e. 11 grid points with $\Delta x = \Delta y = 4.4$ km) is characterized by an energy increase at the scale corresponding to the width of E-zone. A wider E-zone which includes 25 points (i.e. width around 100 km) shows increased energy starting around 100 km. The difference between the impact of the two E-zone widths disappears above about 200 km and under 50 km. Figure 1b additionally illustrates the impact of the selected method,

The impact of periodization on the energy spectra

V. Blažica et al.

Title Page

Abstract

Introduction

Conclusions

References

Tables

Figures



Back

Close

Full Screen / Esc

Printer-friendly Version

Interactive Discussion



order to obtain bi-periodic variations needed for Fourier transforms and spectral space calculations this domain is extended to $N_x \times N_y$ horizontal grid points (Fig. 2).

The current application of ALADIN is based on 11-point E-zones at the northern and eastern boundaries while HIRLAM uses a more flexible extension depending on the actual modelling or assimilation problem. The bi-periodization technique to obtain model field values in the extension zone is only applied for calculation of initial and lateral boundary conditions for the spectral model. During the data assimilation, no bi-periodization is needed since the extension zone is treated like other areas without observations.

The extension of the prognostic fields is performed by using spline (ALADIN) or trigonometric (HIRLAM) functions, which are applied first row by row and second column by column.

The formulas for the row-by-row part in ALADIN are:

$$W_{i,j} = W_{N_{xi},j} + N_j \left(\frac{W_{1,j} - W_{N_{xi},j}}{N} - \frac{N(2M_1 + M_2)}{6} + N_j \left(\frac{M_1}{2} + N_j \frac{M_2 - M_1}{6N} \right) \right) \quad (1)$$

with

$$M_1 = \frac{2Z_1 - \frac{N}{N+1}Z_2}{4 - \left(\frac{N}{N+1}\right)^2}, \quad (2)$$

$$M_2 = \frac{2Z_2 - \frac{N}{N+1}Z_1}{4 - \left(\frac{N}{N+1}\right)^2}, \quad (3)$$

The impact of periodization on the energy spectra

V. Blažica et al.

Title Page	
Abstract	Introduction
Conclusions	References
Tables	Figures
◀	▶
◀	▶
Back	Close
Full Screen / Esc	
Printer-friendly Version	
Interactive Discussion	



and

$$Z_1 = \left(\frac{W_{1,j} - W_{N_{xi},j}}{N} - W_{N_{xi},j} + W_{N_{xi}-1,j} \right) \frac{6}{N+1}, \quad (4)$$

$$Z_2 = \left(W_{1+1,j} - W_{1,j} - \frac{W_{1,j} - W_{N_{xi},j}}{N} \right) \frac{6}{N+1}. \quad (5)$$

5 Here, W is a prognostic variable, N is the width of the extension zone ($N = N_x - N_{xi} + 1$) and N_j is the index of the current point within the extension zone.

For HIRLAM, the formula is:

$$W_{i,j} = g_{j,0} + g_{j,1} \cos 0.5x_i + g_{j,2} \sin 0.5x_i + g_{j,3} \sin x_i, \quad (6)$$

10 where $x_i = \frac{2\pi(i-N_{xi})}{N}$ and the coefficients $g_{j,k}$ ($k = 0, 1, 2$ and 3) are determined to make the extrapolation expression fit the original grid-point values exactly for $i = 1, 2, -1$ and N_{xi} .

In ALADIN, solutions over the extension zone are additionally smoothed by a two-dimensional 9-point weighted average for each point in the E-zone. One motivation for the smoothing was the removal of small scale dynamical features in the interior domain that are reflections of small scale features in the extension zone caused by the isotropic truncation.

Because the E-zone is considered to have a negligible impact on model calculations, it is usually included in the kinetic energy spectra of dynamical fields and in the spectra of the forecast-error variances used in data assimilation. As discussed in Blažica et al. (2013), the kinetic energy spectra with the extension zone included are regularly used in ALADIN and HIRLAM studies of the model performance (e.g., Horvath et al., 2011) and for tuning of the model numerics (e.g., Váňa et al., 2008) and physics (e.g., Bengtsson et al., 2012).

25 In the HIRLAM model application, imbalances in the extension zone as a possible source of problems for the initialization are treated by geostrophic balancing of the

The impact of periodization on the energy spectra

V. Blažica et al.

Title Page

Abstract

Introduction

Conclusions

References

Tables

Figures



Back

Close

Full Screen / Esc

Printer-friendly Version

Interactive Discussion



gravest vertical modes (tendencies of the fastest gravity modes are put to zero). In HIRLAM, the extension is carried out for the lateral boundary data only.

2.2 The extension zone – the Boyd window method

The Boyd method (Boyd, 2005) is another method that uses the extension zone, but instead of applying a spline or a trigonometric periodization operator, the method makes use of the prognostic variable values from outside the model domain. This is not seen as a problem because periodization is done on the data from the host model. The Boyd method can be seen as a decrease in size of the extension zone, but the transition from the solution on one side of the domain to the solution on the other side still introduces some aliasing.

The values in the extended area are a combination of the additional values beyond the eastern/northern boundary and the additional values beyond the western/southern boundary. The transition between the two is achieved by a windowing function (Termo-
nia et al., 2012):

$$B_x = \begin{cases} 0 & \text{for } |x| \geq 2\Theta - \chi \\ \frac{1}{2} + \frac{1}{2} \left[\frac{L}{2} \frac{(2\Theta - \chi - |x|) - (|x| - \chi)}{(2\Theta - \chi - |x|)(|x| - \chi)} \right] & \text{for } \chi < |x| < 2\Theta - \chi \\ 1 & \text{for } |x| \leq \chi \end{cases} \quad (7)$$

Here the interval to be periodized is $[-\Theta, \Theta]$, the physical domain is limited to the smaller interval $[-\chi, \chi]$, L is a tunable parameter (in our experiment set to 1.6) and erf is the error function. The variable is first multiplied with the windowing function and next a summation of the shifted products is performed:

$$W'(x) = \sum_{k=-\infty}^{\infty} B(x + 2k\Theta)W(x + 2k\Theta). \quad (8)$$

The impact of periodization on the energy spectra

V. Blažica et al.

Title Page

Abstract

Introduction

Conclusions

References

Tables

Figures



Back

Close

Full Screen / Esc

Printer-friendly Version

Interactive Discussion



This method has recently been adapted to the ALADIN code and can now be run operationally. Its performance in the HARMONIE model was demonstrated by Termonia et al. (2012) and Degrauwe et al. (2012), who showed that the Boyd method outperforms the spline-based periodization method, especially in the cases of strong dynamical forcing at the lateral boundaries. This suggests that the method applied to make fields periodic has an impact on the model performance although the reasons are not clear.

2.3 The detrending method

The detrending method (Errico, 1985, 1987) removes the scales that are larger than represented by the limited domain and thus not resolved. It consists of the computation of the linear trend between the end points along each row and column of data, followed by the removal of the trend:

$$s_j = \frac{W_{N_{xi},j} - W_{1,j}}{N_{xi} - 1} \quad (9)$$

$$W'_{i,j} = W_{i,j} - \frac{1}{2}(2i - N_{xi} - 1)s_j \quad (10)$$

Here, s_j denotes the linear trend and W' is the modified field. The procedure matches the first and the last point of the row/column, thus making the fields periodic. The manipulated field usually contains a pattern of lines, created by the linear treatment. As mentioned by the author, the method should not be used if the fields are noisier at the boundaries than in the interior of the domain.

The detrending method has been widely used to estimate the spatial spectra of limited-area models (e.g., Van Tuyl and Errico, 1989; Skamarock, 2004; Frehlich and Sharman, 2008; Bierdel et al., 2012). Additionally, it is regularly implemented when producing the spectra of time series (e.g., Termonia, 2008; Termonia et al., 2009).

The impact of periodization on the energy spectra

V. Blažica et al.

Title Page

Abstract

Introduction

Conclusions

References

Tables

Figures



Back

Close

Full Screen / Esc

Printer-friendly Version

Interactive Discussion



2.4 The discrete cosine transform

The discrete cosine transform (Ahmed et al., 1974; Denis et al., 2002) is a method most commonly used for image processing. The periodization is achieved by adding a mirror image to the variable field. Due to the even symmetry of the created field, the Fourier transform consists only of the cosine functions, hence the name of the method.

The periodic function is constructed by taking the position $j = -1/2$ as a mirror:

$$W(i) = \begin{cases} W(i) & \text{for } i \geq 0 \\ W(-1 - i) & \text{for } i < 0 \end{cases} \quad (11)$$

Discrete Fourier transform is then applied to the new function, centred on $i = -1/2$.

While this transform method is widely used for compression of digital images, its use for atmospheric spectral analysis has only recently received attention. It has been for example applied to obtain the ALADIN kinetic energy spectra in Ricard et al. (2013) and Brousseau et al. (2012).

2.5 Demonstration of the above methods

For a demonstration of the periodization procedure, all the methods were applied to an arbitrary field with a small domain and a large extension zone (60×60 grid points, with 18 points in the extension zone). Figure 3 demonstrates periodization of one grid-point line for each of the discussed methods. The two-dimensional prognostic fields after the application of the periodization methods are presented in Figs. 4 and 5.

The properties of the fields with the Boyd and detrending methods for periodization look similar to the original field (top left in Fig. 4) while the HIRLAM and ALADIN methods produce patterns along rows and columns of the E-zone (which are partially omitted after the ALADIN smoothing procedure) and an area with absolute maximum in the top right corner of the domain (where the values are obtained after extrapolation in both horizontal directions). Both phenomena impact the spectra, as will be shown below.

physical field. After the application of the selected method for periodization, the fields are transformed back to spectral space by a two-dimensional direct FFT and their new kinetic energy spectrum is compared to the original one.

Note that the simulation method favours the detrending method with nearly no trend to be removed. In reality, fields can have a large trend (e.g. north-to-south temperature gradient, wind gradient when a trough enters the domain etc.) and detrending could produce a much larger effect. The simulation method to some extent also favours the Boyd method since grid-point values obtained from the “true” spectrum are used in the extension zone. This is not possible in a real case where the host model grid-point values, obeying the spectrum of the host model, are utilized.

4 The impact of periodization on the kinetic energy spectrum

In this section we discuss the kinetic energy spectra for all the above mentioned methods. The methods are named after the models that use them. The results, based on averaging over 500 realizations of the random wind field, are depicted in Fig. 6. For the methods that make use of the extension zone, the spectra for two different widths of the extension zone (18 and 48 grid points) are presented. For the ALADIN model, we show two sets of spectra – one after the spline function periodization (referred to as ALADIN) and the other after applying the smoothing to the periodized fields (as done operationally; referred to as ALADIN SMOOTH).

The resulting spectra show significant differences among the methods under investigation. While the Boyd and the detrending method remain very close to the original spectrum, there is a significant increase of the energy for the ALADIN and HIRLAM methods. The similar shapes of spectra for these two methods show that the deformation is mainly a consequence of the extension zone geometry and not of the function used for the periodization. For the extension zone width of 18 grid points the added (excess) energy increases gradually towards shorter scales. For the 48-point zone, this process is also observed, but the most distinctive feature of the spectra is a bump,

The impact of periodization on the energy spectra

V. Blažica et al.

Title Page

Abstract

Introduction

Conclusions

References

Tables

Figures



Back

Close

Full Screen / Esc

Printer-friendly Version

Interactive Discussion



centred approximately at wavenumber 8 with an amplitude about one order of magnitude larger than for the original spectrum. A more careful inspection reveals that a very small bump can already be seen in the 18-point E-zone for the HIRLAM method, centred at about wavenumber 25. We investigate the location, amplitude and cause of this phenomenon later in the paper.

In the wide extension zone, the ALADIN SMOOTH spectrum first follows the ALADIN spectrum in the bump region, but descends from it and approaches the original spectrum at about wavenumber 50. Towards the shortest scales (at about wavenumber 60), the amplitude of the spectrum becomes even smaller than the original $k^{*-5/3}$ because the smoothing operator filters out some of the short-scale waves. The spectrum slope of the ALADIN SMOOTH method is thus steeper than the original one. The curve resembles Fig. 1, where the ALADIN SMOOTH method was applied to real forecast fields.

Figure 7 shows the ratio between the computed spectra and the prescribed $k^{*-5/3}$ spectrum for the detrending method, the DCT, and for several widths of the extension zone for the Boyd method. At large scales, all spectra contain energy which exceeds the energy of the original field. All methods provide spectra that slowly approach the prescribed spectrum as scales become shorter. The energy ratio remains stable for wavenumbers above 30. The spectrum of the detrending method remains above the amplitude of $k^{*-5/3}$ spectrum at all scales while the Boyd method loses some of the initial energy, depending on the size of the extension zone. The best match to the original spectra presents the DCT method. The differences among the spectra are small compared to the impact of the ALADIN and HIRLAM methods, on which we focus next.

For the HIRLAM and ALADIN methods, the spectra with several widths of the extension zone are shown in Fig. 8. The deformation of the spectra increases and moves upscale with increasing size of the E-zone, supporting the use of a narrow extension zone for a smaller impact on the spectra. The location of the bump shifts nearly linearly towards smaller wavenumbers. This confirms that the location of the bump is closely

The impact of periodization on the energy spectra

V. Blažica et al.

Title Page

Abstract

Introduction

Conclusions

References

Tables

Figures



Back

Close

Full Screen / Esc

Printer-friendly Version

Interactive Discussion



related to the width of the extension zone. The ALADIN SMOOTH spectra resemble the ALADIN spectra at large scales, but the energy decreases significantly for shorter scales due to the smoothing effect.

A similar ratio as in Fig. 7 is shown in Fig. 9 for the HIRLAM and ALADIN spectra.

Because for these two methods there are no special requests for the size of the extension zone, periodization was done for 25 widths, from 0 to 216 grid points, increasing the width of the extension zone by 8 grid points. The size of the extension zone in percentages of the full field is shown on y axis. While such large sizes of the extension zone are not used in practice, these plots emphasize the importance of the extension zone width to the location of the spectral bump and to an overall deformation of the spectrum.

To further investigate the large energy values in the ALADIN and HIRLAM spectra, we perform row-wise one-dimensional FFT's in the x direction. Thus obtained spectra are averaged over rows 1 to N_{yi} (384) separately and over rows $N_{yi} + 1$ (385) to N_y (432) separately (see Fig. 10). The former spectra mainly contain the information in physical space with only the last 48 points of each row in the extension zone and should thus enclose the effect of periodization in single rows. The latter spectra on the other hand only contain the information in the extension zone and should enclose the effect of performing periodization line-by-line. Additionally, these spectra also include large values of the extended fields in the top right corner (see Fig. 4).

Averaging the one-dimensional spectra in the physical field (with only the last 48 grid points reaching into the extension zone) shows that the added energy only occurs at scales larger than the width of the extension zone (Fig. 11). The reason for this is that the spline or trigonometric functions complete the series of data with shapes varying from a single wave towards a flat line, which therefore projects the added energy on the scales which correspond to waves with scales larger than the extension zone width. Smoothing the ALADIN method fields further reduces the added energy.

Averaging over the rows in the extension zone gives much larger amplitudes of the spectra across all scales. The large scale contribution is higher than in the previous

The impact of periodization on the energy spectra

V. Blažica et al.

Title Page

Abstract

Introduction

Conclusions

References

Tables

Figures



Back

Close

Full Screen / Esc

Printer-friendly Version

Interactive Discussion



The impact of periodization on the energy spectra

V. Blažica et al.

Title Page

Abstract

Introduction

Conclusions

References

Tables

Figures



Back

Close

Full Screen / Esc

Printer-friendly Version

Interactive Discussion



case and it is not affected by the smoothing operator. We assume that the cause is the top right corner of the extended domain, which was not included in the physical-field spectra. There is also some additional energy towards shorter scales, which was not present in averaging in physical space. This small-scale part of the spectra most likely comes from the line-by-line periodization (extrapolation), the effect of this was not present in the physical-field spectra. This shorter-scale excess energy is however efficiently removed by applying the smoothing filter in ALADIN SMOOTH.

The analysis of one-dimensional spectra obtained by the ALADIN and HIRLAM methods enables us a valuable insight into the structure of the spectra. We showed that the bump in the spectra at large scales occurs for two reasons: one is the periodization function, which completes the data with shapes that vary from one wave to a flat line; the other is the extreme values in the top right corner of the periodized domain, which only influence in the spectra in the extension zone. The short-scale excess energy comes from row-by-row and column-by-column periodization of the variables. The smoothing operator efficiently filters out the short-scale noise and some of the large-scale energy.

The geometry of the domain in this experiment is very similar to the ALADIN model setup shown in the introduction. Comparison of these simple spectra to the spectra of real forecast fields where the ALADIN SMOOTH method was applied helps to interpret the results with the real fields: the smoothing operator efficiently removes the excess short-scale energy, added by the extension zone, and for this reason the spectra of extension zone method and the spectra of the detrending method match below the scales of 50 km. The large-scale bump, originating from the treatment of the top right corner of the domain, however still remains, and causes the deviation of the extension zone spectra from the detrended spectra.

The impact of periodization on the energy spectra

V. Blažica et al.

Title Page

Abstract

Introduction

Conclusions

References

Tables

Figures



Back

Close

Full Screen / Esc

Printer-friendly Version

Interactive Discussion



- While the impact of the HIRLAM and ALADIN periodization is nearly unnoticeable for physical fields with narrow extension zones that have large amplitudes of energy at scales affected by the E-zone (for instance the fields in planetary boundary layer), the latter is not the case in the stratosphere, as seen for operational model's kinetic energy spectra in Fig. 1.
- The original HIRLAM and ALADIN algorithms should not be applied for calculation of spectra with wide extension zones since the constraint on preservation of normal gradients together with the selected extrapolation functions leads to strong amplification of variations in the extension zone.

Acknowledgements. We thank our ALADIN colleagues Daan Degrauwe, Benedikt Strajnar, Jure Cedilnik and Antonio Stanešić for their assistance with information and code on different periodization methods. Jelena Bojarova and Magnus Lindskog provided insight and expertise that greatly assisted the research. Research of Nedjeljka Žagar is supported by the funding from the European Research Council, Grant Agreement no. 280153.

References

- Ahmed, N., Natarajan, T., and Rao, K. R.: Discrete cosine transform, *IEEE T. Comput.*, C-23, 90–93, 1974. 6492, 6498
- Bengtsson, L., Tijm, S., Váňa, F., and Svensson, G.: Impact of flow-dependent horizontal diffusion on resolved convection in AROME, *J. Appl. Meteorol. Clim.*, 51, 54–67, 2012. 6495
- Bierdel, L., Friederichs, P., and Bentzien, S.: Spatial kinetic energy spectra in the convection-permitting limited area NWP model COSMO-DE, *Meteorol. Z.*, 21, 245–258, 2012. 6497
- Blažica, V., Žagar, N., Strajnar, B., and Cedilnik, J.: Rotational and divergent kinetic energy in the mesoscale model ALADIN, *Tellus A*, 65, 18918, doi:10.3402/tellusa.v65i0.18918, 2013. 6491, 6495
- Boyd, J. P.: Limited-area Fourier spectral models and data analysis schemes: windows, Fourier extension, Davies relaxation, and all that, *Mon. Weather Rev.*, 133, 2030–2042, 2005. 6492, 6496

The impact of periodization on the energy spectra

V. Blažica et al.

Title Page

Abstract

Introduction

Conclusions

References

Tables

Figures



Back

Close

Full Screen / Esc

Printer-friendly Version

Interactive Discussion



- Brousseau, P., Berre, L., Bouttier, F., and Desroziers, G.: Flow-dependent background-error covariances for a convective-scale data assimilation system, *Q. J. Roy. Meteor. Soc.*, 138, 310–322, 2012. 6492, 6498
- 5 Degrauwe, D., Caluwaerts, S., Voitus, F., Hamdi, R., and Termonia, P.: Application of Boyd's periodization and relaxation method in a spectral atmospheric limited-area model. Part II: Accuracy analysis and detailed study of the operational impact, *Mon. Weather Rev.*, 140, 3149–3162, 2012. 6492, 6497
- Denis, B., Côté, J., and Laprise, R.: Spectral decomposition of two-dimensional atmospheric fields on limited-area domains using the discrete cosine transform (DCT), *Mon. Weather Rev.*, 130, 1812–1829, 2002. 6492, 6498
- 10 Errico, R. M.: Spectra computed from a limited-area grid, *Mon. Weather Rev.*, 113, 1554–1562, 1985. 6492, 6497
- Errico, R. M.: A comparison between two limited-area spectral analysis schemes, *Mon. Weather Rev.*, 115, 2856–2861, 1987. 6497
- 15 Frehlich, R. and Sharman, R.: Estimates of turbulence from numerical weather prediction model output with applications to turbulence diagnosis and data assimilation, *Mon. Weather Rev.*, 132, 2308–2324, 2004. 6491
- Frehlich, R. and Sharman, R.: The use of structure functions and spectra from numerical model output to determine effective model resolution, *Mon. Weather Rev.*, 136, 1537–1553, 2008. 6491, 6497
- 20 Haugen, J. E. and Machenhauer, B.: A spectral limited-area model formulation with time-dependent boundary conditions applied to the shallow-water equations, *Mon. Weather Rev.*, 121, 2618–2630, 1993. 6492, 6493
- Horvath, K., Bajić, A., and Ivatek-Šahdan, S.: Dynamical downscaling of wind speed in complex terrain prone to bora-type flows, *J. Appl. Meteorol. Clim.*, 50, 1676–1691, 2011. 6495
- 25 Lindborg, E.: Can the atmospheric kinetic energy spectrum be explained by two-dimensional turbulence?, *J. Fluid Mech.*, 388, 259–288, 1999. 6490
- Nastrom, G. D. and Gage, K. S.: A climatology of atmospheric wavenumber spectra of wind and temperature observed by commercial aircraft, *J. Atmos. Sci.*, 42, 950–960, 1985. 6490
- 30 Ricard, D., Lac, C., Riette, S., Legrand, R., and Mary, A.: Kinetic energy spectra characteristics of two convection-permitting limited-area models AROME and Meso-NH, *Q. J. Roy. Meteor. Soc.*, 139, 1327–1341, 2013. 6492, 6498

The impact of periodization on the energy spectra

V. Blažica et al.

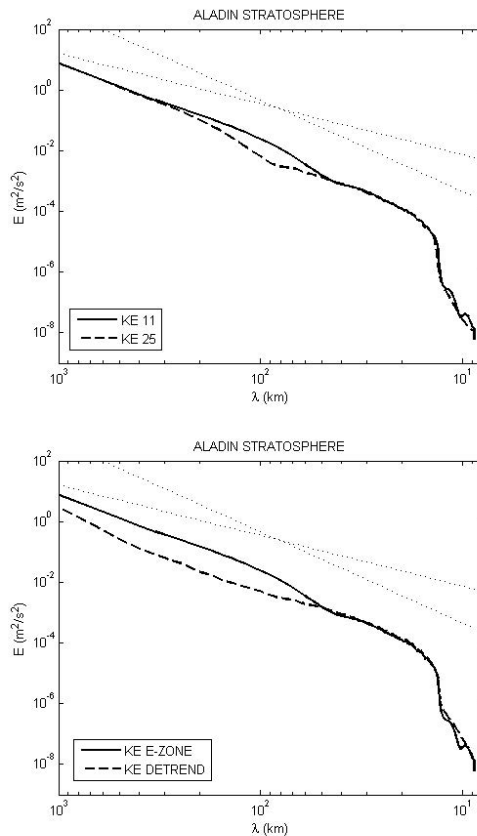


Figure 1. Kinetic energy spectra of the ALADIN/SI model with 4.4 km horizontal resolution, averaged over model levels between 5 and 250 hPa. Top: Comparison of ALADIN spectra with 11 and 25 points in the E-zone. Bottom: Comparison of ALADIN detrended spectra and spectra with E-zone.

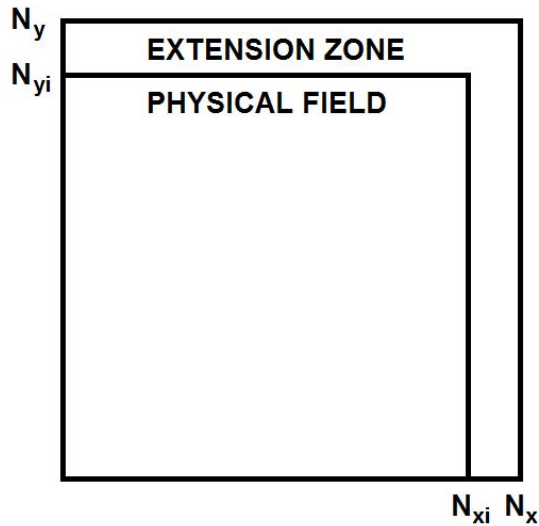


Figure 2. A typical setup of the NWP model domain with the extension zone.

**The impact of
periodization on the
energy spectra**

V. Blažica et al.

Title Page

Abstract Introduction

Conclusions References

Tables Figures

◀ ▶

◀ ▶

Back Close

Full Screen / Esc

Printer-friendly Version

Interactive Discussion



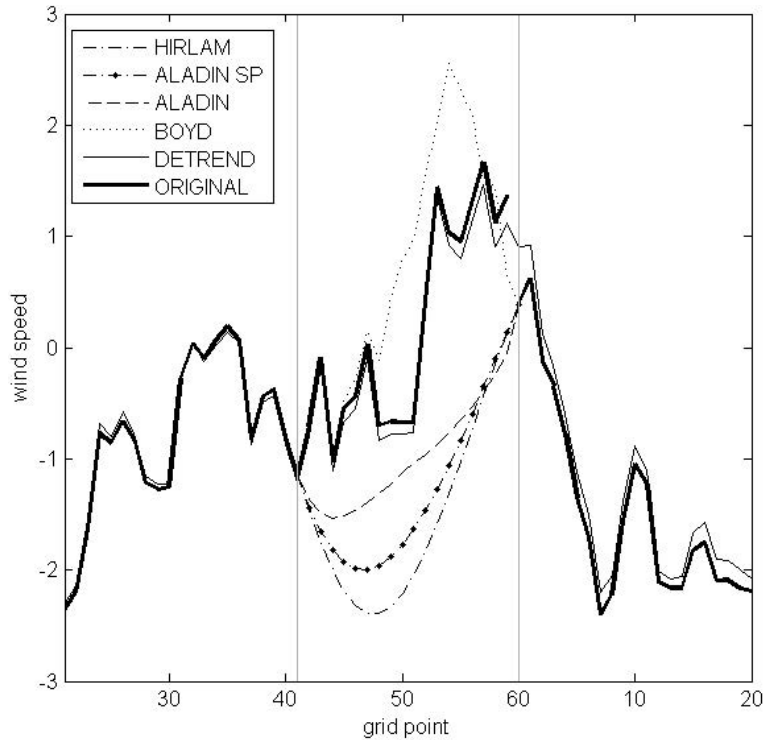


Figure 3. One-dimensional periodization of an arbitrary wind field for the discussed methods except for DCT. The thin grey lines denote the borders of the extension zone.

The impact of periodization on the energy spectra

V. Blažica et al.

[Title Page](#)

[Abstract](#) | [Introduction](#)

[Conclusions](#) | [References](#)

[Tables](#) | [Figures](#)

[◀](#) | [▶](#)

[◀](#) | [▶](#)

[Back](#) | [Close](#)

[Full Screen / Esc](#)

[Printer-friendly Version](#)

[Interactive Discussion](#)



The impact of periodization on the energy spectra

V. Blažica et al.

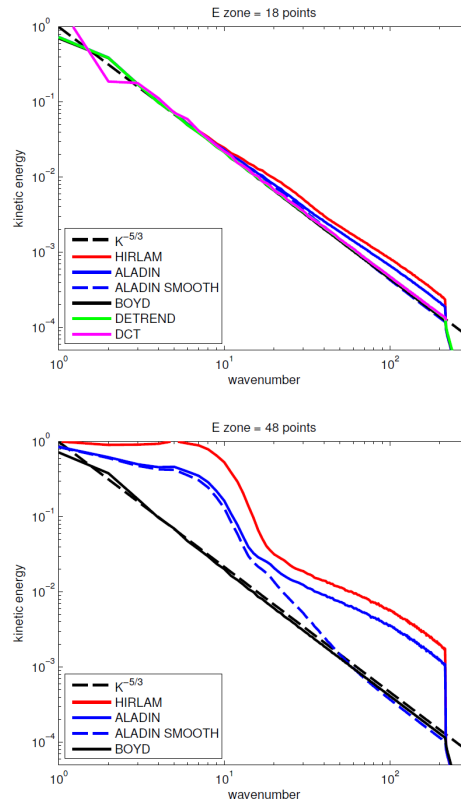


Figure 6. Kinetic energy spectra for all the discussed techniques. The results with two widths of the extension zone are presented for HIRLAM, ALADIN and Boyd methods: a narrower one with 18 points (top) and a wider one with 48 points (bottom).

[Title Page](#)
[Abstract](#)
[Introduction](#)
[Conclusions](#)
[References](#)
[Tables](#)
[Figures](#)
[◀](#)
[▶](#)
[◀](#)
[▶](#)
[Back](#)
[Close](#)
[Full Screen / Esc](#)
[Printer-friendly Version](#)
[Interactive Discussion](#)


The impact of periodization on the energy spectra

V. Blažica et al.

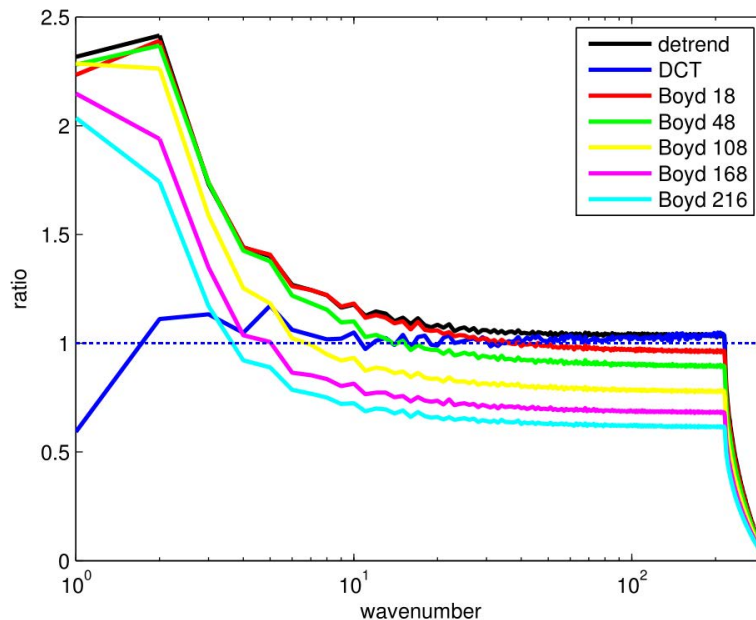


Figure 7. The ratio between the computed spectrum and the prescribed $k^{-5/3}$ spectrum for the detrending method, the discrete cosine transform and the Boyd method for several widths of the extension zone.

[Title Page](#)
[Abstract](#)
[Introduction](#)
[Conclusions](#)
[References](#)
[Tables](#)
[Figures](#)
[◀](#)
[▶](#)
[◀](#)
[▶](#)
[Back](#)
[Close](#)
[Full Screen / Esc](#)
[Printer-friendly Version](#)
[Interactive Discussion](#)


The impact of periodization on the energy spectra

V. Blažica et al.

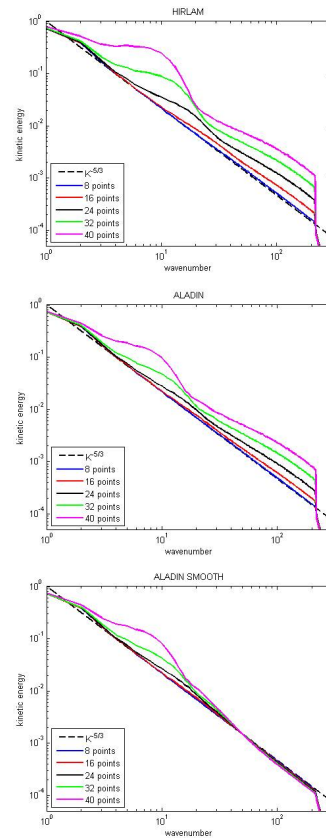


Figure 8. Kinetic energy spectra for HIRLAM (top), ALADIN (middle) and ALADIN SMOOTH (bottom) methods for several widths of the extension zone.

[Title Page](#)
[Abstract](#)
[Introduction](#)
[Conclusions](#)
[References](#)
[Tables](#)
[Figures](#)
[⏪](#)
[⏩](#)
[◀](#)
[▶](#)
[Back](#)
[Close](#)
[Full Screen / Esc](#)
[Printer-friendly Version](#)
[Interactive Discussion](#)


The impact of periodization on the energy spectra

V. Blažica et al.

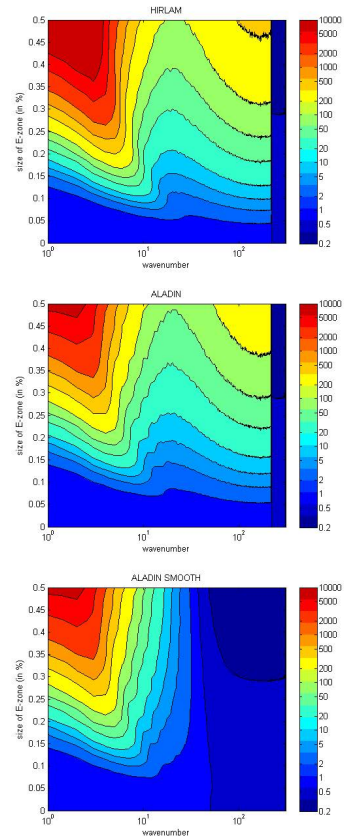


Figure 9. The ratio between the periodized spectrum and the original $k^{-5/3}$ spectrum for several widths of the extension zone for HIRLAM (top), ALADIN (middle) and ALADIN SMOOTH (bottom) methods. The ratio between the size of the extension zone and the full domain is shown on y axis.

[Title Page](#)
[Abstract](#)
[Introduction](#)
[Conclusions](#)
[References](#)
[Tables](#)
[Figures](#)
[⏪](#)
[⏩](#)
[◀](#)
[▶](#)
[Back](#)
[Close](#)
[Full Screen / Esc](#)
[Printer-friendly Version](#)
[Interactive Discussion](#)


The impact of periodization on the energy spectra

V. Blažica et al.

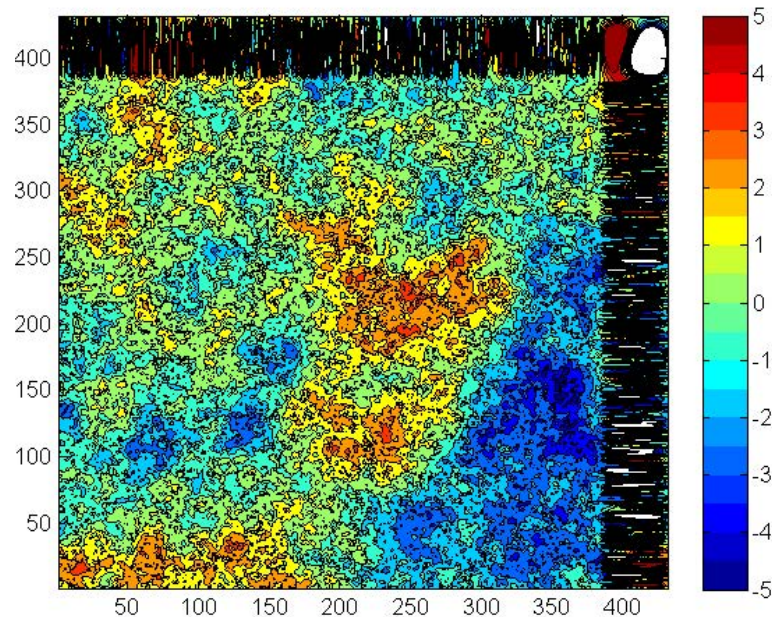


Figure 10. An arbitrary grid-point field with $N_{x_i} = N_{y_i} = 432$ and the extension zone width of 48 points, periodized with the HIRLAM method.

[Title Page](#)[Abstract](#)[Introduction](#)[Conclusions](#)[References](#)[Tables](#)[Figures](#)[◀](#)[▶](#)[◀](#)[▶](#)[Back](#)[Close](#)[Full Screen / Esc](#)[Printer-friendly Version](#)[Interactive Discussion](#)

The impact of periodization on the energy spectra

V. Blažica et al.

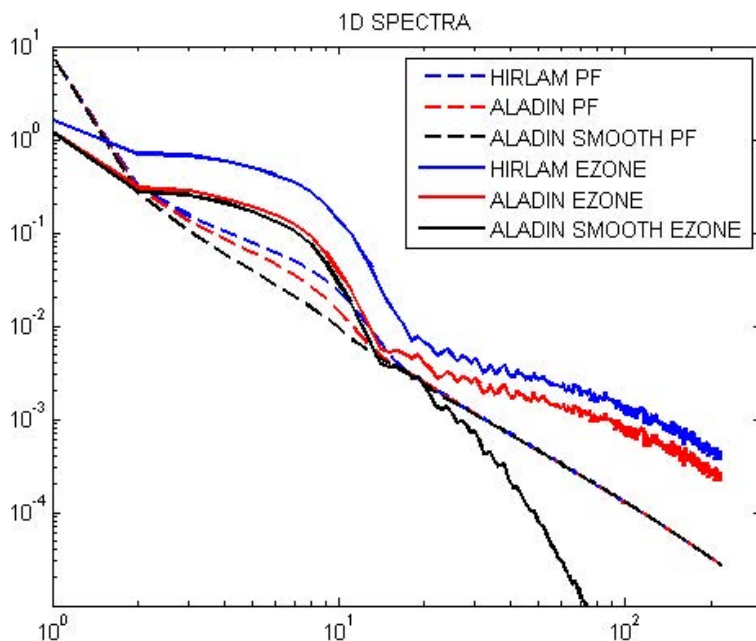


Figure 11. Average one-dimensional spectra only in the extension zone (EZONE, solid lines) and only in the physical field (PF, dashed lines) for HIRLAM, ALADIN and ALADIN SMOOTH methods.

Title Page

Abstract

Introduction

Conclusions

References

Tables

Figures

◀

▶

◀

▶

Back

Close

Full Screen / Esc

Printer-friendly Version

Interactive Discussion

